JOURNAL OF CATALYSIS 79, 359–377 (1983)

Surface Characterization of Ammonia Synthesis Catalysts

G. ERTL AND D. PRIGGE

Institut für Physikalische Chemie, Universität München, München, West Germany

R. SCHLOEGL

Institut für Anorganische Chemie, Universität München, München, West Germany

AND

M. WEISS

Perkin–Elmer Verkauf GmbH, Physical Electronics Division Europe, München-Vaterstetten, West Germany

Received July 23, 1982; revised October 7, 1982

Composition and topography of the surfaces of unreduced and reduced industrial ammonia synthesis catalysts (BASF S6-10) were investigated by means of scanning Auger electron spectroscopy, X-ray photoelectron spectroscopy, and scanning electron microscopy. The unreduced samples exhibit strong surface segregation and rather nonuniform lateral distribution of the promoter elements (Al, K, Ca); no pores with diameter $\lesssim$1000 Å are present. After reduction a network of particles and pores with diameters in the range between 100 and 500 Å can be observed which visualizes the pronounced increase of the surface area due to the presence of the structural promoter Al_2O_3 (+ CaO). Reduction transforms Fe completely into its metallic state. The iron particles are uniformly covered by a K + O adlayer which acts as "electronic" promoter. Previous reports in the literature on the surface properties of ammonia synthesis catalysts, which were based on more indirect methods (selective adsorption, etc.), are in full qualitative accordance with the present conclusions.

1. INTRODUCTION

Since the discovery of the doubly promoted iron catalyst for ammonia synthesis more than 70 years ago (*1*) numerous investigations on the characterization of these catalysts have been performed (*2*). Earlier studies yielded mostly indirect information, e.g., on the basis of surface area and selective adsorption experiments (*3–9*) which were supplemented by experiments using transmission electron microscopy (TEM) (*10, 11*) and electron microprobe analysis (*12*), providing insight into the pore structure and the nonuniform distribution of the elements, respectively. X-Ray diffraction (*13–17*) and Mössbauer spectroscopy (*18, 19*) served for elucidating the crystallographic structure of the catalyst particles and the chemical nature of the (bulk) iron. More recently the first reports on the direct probing of the *surface* properties by means of surface spectroscopic techniques appeared in the literature: Buhl and Preisinger (*20*) recorded the ions sputtered from a reduced $Fe–Al_2O_3$ catalyst by means of secondary ion mass spectroscopy (SIMS). Ertl and Thiele (*21*) investigated the composition and the oxidation state of the elements in the surface region of an industrial catalyst (BASF S6-10) as well as the changes caused by reduction by means of X-ray photoelectron spectroscopy (XPS). Hanji *et al.* (*22*) applied Auger electron spectroscopy to surface analysis of doubly and triply promoted catalysts and reported (qualitatively) observations of nonuniformities in the lateral distributions of various elements on the surface.

The present paper follows this latter ap-

0021-9517/83/020359-19$03.00/0

proach and reports on the results of a detailed study on the surface properties of the same industrial catalyst as used in the previous XPS work from this laboratory (*21*). In addition to XPS the techniques of scanning electron microscopy (SEM) and scanning Auger electron spectroscopy (SAES) were used for characterizing the topography as well as the laterally resolved composition of the surface. The conclusions to be reached will be in almost complete agreement with those based on previous investigations using more indirect methods. Apart from confirming the picture of one of the most important industrial catalysts this agreement is also considered in a more general sense as a justification of the "classical" techniques used in catalyst characterization, such as selective chemisorption, etc.

2. EXPERIMENTAL

In situ experiments (in which the catalyst could be reduced or exposed to various atmospheres at pressure up to 1 atm and subsequently analyzed under ultrahigh-vacuum conditions) were performed with an XPS system as already used in the previous cited work (*21*). For the SEM and SAES measurements the reduced catalyst had to be transported through air, thus causing superficial reoxidation of the iron particles without affecting, however, the pore structure nor the lateral distribution of the promoter elements.

For scanning electron microscopy a Camscan (Kontron) system was used. With thoria-coated tungsten filaments operated at 25 keV with a 150-μA beam current a lateral resolution of better than 100 Å can be reached. The conductivity of the reduced catalyst samples was sufficiently high so that only very slight sputtering with gold was needed. The unreduced samples, however, required sputtering with both gold and carbon in order to obtain good images at high magnifications. Possible artifacts introduced in this way could be recognized by subsequent sputtering of an approximately 50-Å-thick layer at random orientation of the sample with intermittent observation: prior to the visibility of erosion small gold droplets could be detected, which were identified with an X-ray dispersive spectrometer attached to the microscope system.

For scanning Auger electron spectroscopy a PHI 590 SAM system (lateral resolution about 2000 Å) was used in the case of the unreduced samples, while for the reduced catalysts a PHI 595 SAM system (best lateral resolution about 500 Å) was available. These systems also permitted us to record secondary electron images (beam energy 10 keV) from the area to be analyzed by SAES so that lateral variations in the surface composition, as become evident from the "Auger maps," could be correlated with corresponding features in the surface topography. Since the formation of these secondary electron images occurs through the same mechanism as in the scanning electron microscope, the information from both techniques can be directly compared with each other. Quantitative evaluation of the surface composition from AES data was achieved by recording the peak-to-peak amplitude of the respective element and by using the corresponding sensitivity factors (*23*) and through calibration with practically pure particles of Al_2O_3, CaO, and K_2O on the catalyst surface. The XPS data were analyzed by using tabulated ionization cross sections for the corresponding levels of the various elements (*24*). Both techniques are, of course, not only probing the topmost atomic layer but a region of about 10 to 20 Å in depth (depending on the energy of the electrons used for the analysis), and therefore the indicated compositions refer to this "surface region."

The experiments were performed with crushed pieces of BASF S6-10 catalyst (approximate dimensions $8 \times 5 \times 3$ mm^3) without any further flattening or polishing. The (macroscopic) surface roughness is only of minor importance with respect to the conclusions to be reached.

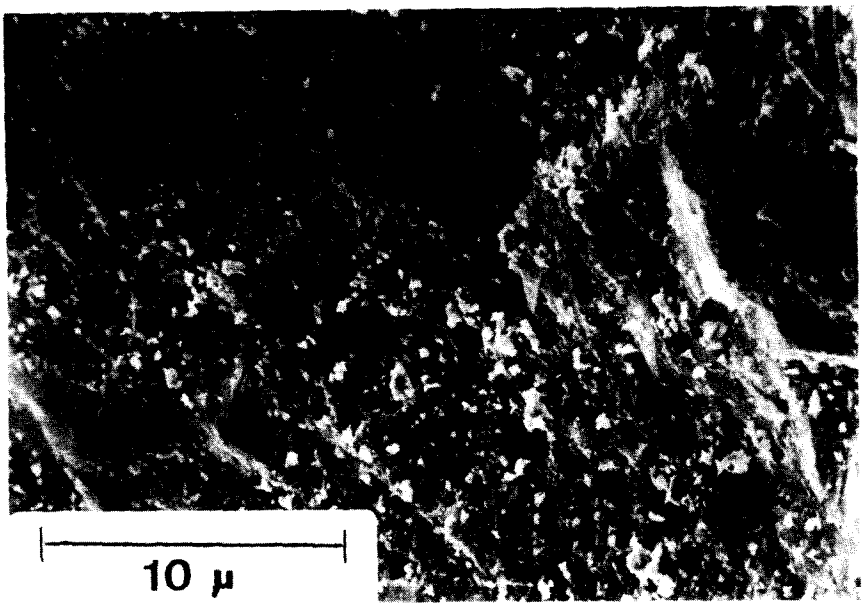

FIG. 1. Scanning electron microscope (SEM) image from a characteristic surface area of the unreduced catalyst.

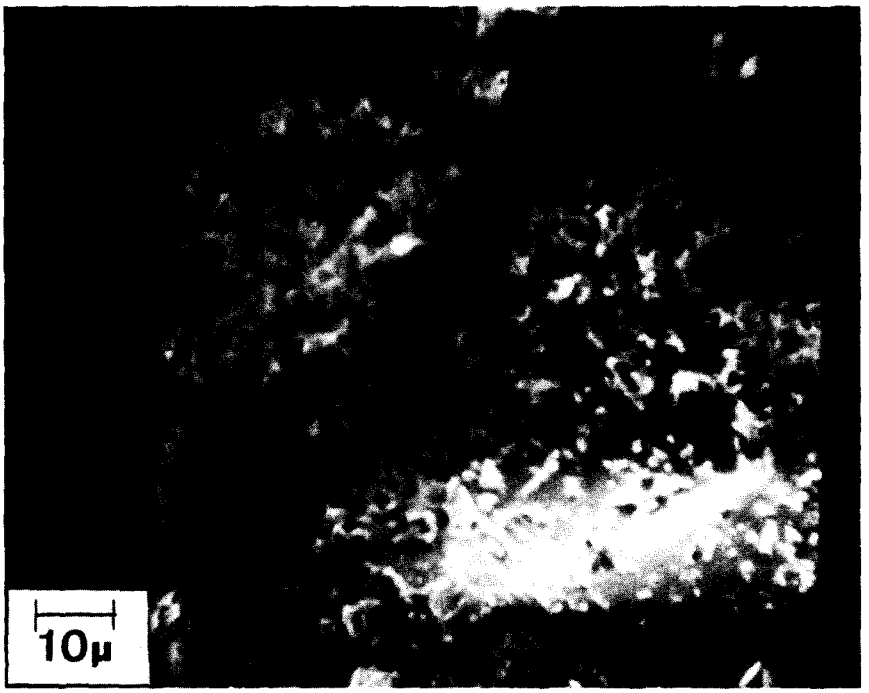

FIG. 2. Secondary electron distribution (SED) image recorded with the Auger spectrometer from a typical area of the unreduced catalyst. The results of local AES analysis of the points 1–3 are listed in Table 1.

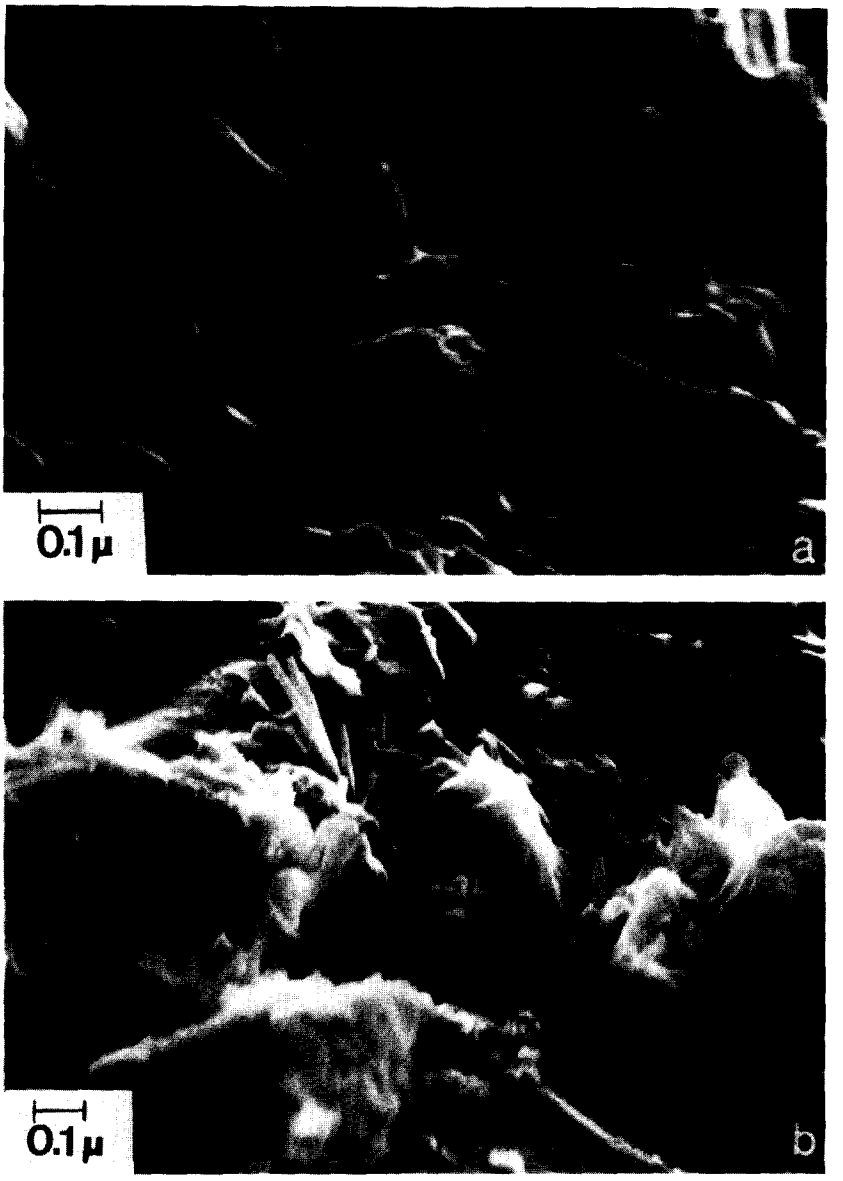

FIG. 3. High-magnification SEM images from two selected typical areas of the unreduced catalyst.

3. RESULTS

3.1. Unreduced Catalyst

The ammonia synthesis catalyst is prepared by oxidative fusion of iron with the promoter oxides at temperatures above 1800K. Upon cooling rather large magnetite (Fe_3O_4) crystals are formed in which Al_2O_3 and CaO are dissolved, forming spinel structures. Potassium is most likely segregating at the grain boundaries (*2*).

Figure 1 shows a scanning electron micrograph of such a catalyst particle with relatively low magnification. For comparison a secondary electron image recorded with the SAES apparatus with similar magnification is reproduced in Fig. 2. This same part of the surface area will be analyzed in all

the following Auger experiments, so that the resulting features may be directly correlated with the surface topography.

SEM images with high magnification are reproduced in Fig. 3. The essential point is that structures with pores of diameters in the 100-Å range are never observed. The surfaces are rather smooth and are covered with small crystallites (Fig. 3b) consisting of segregated promoter oxides.

The lateral distributions of the four elements Fe, K, Al, and Ca over the surface area reproduced in Fig. 2 become qualitatively evident from the "Auger maps" of Fig. 4. Here the brightness is a relative measure of the local surface concentration, i.e., dark areas denote low concentration of the respective element. The elemental distribution is rather inhomogeneous, even on this scale. Relatively large Fe areas, forming the flat portions in Fig. 2, are free from Ca, and contain relatively little Al, but substantial amounts of K. It is further important to note that K is not yet uniformly spreading over the Fe areas.

The bulk composition of the unreduced catalyst is compared in Table 1 with the surface compositions for a large surface area (~0.5 cm^2) as determined by XPS (b), with the integral composition of the area shown in Figs. 2 and 4 (ca. 10^{-4} cm^2) as derived from AES (c) and for selected points marked in Fig. 2 (analyzed area about 10^{-8} cm^2) (d–f). The XPS data are within the limits of the data for various samples as reported in Ref. (*21*), with the exception of K, which is even larger in the present case. For the evaluation of these numbers the carbon content was not taken into account, which arises essentially as an impurity from the vapors of the pumping system, but which is most likely associated with potassium in the form of K_2CO_3. Essentially no carbon signal was found with the Auger spectra: here the vacuum system is only operated with ion pumps and K_2CO_3 most probably decomposes under the influence of the electron beam into $K_2O + CO_2$.

TABLE 1

Composition of the Unreduced Catalyst (at%)

	Fe	K	Al	Ca	O
(a) Bulk composition (BASF S6-10)	40.5	0.35	2.0	1.7	53.2
(b) XPS—total surface	3.2	33.2	8.4	3.9	51.3
(c) AES—area of Fig. 2	8.6	36.1	10.7	4.7	40
(d) AES—point 1 of Fig. 2	27.3	22.6	4.2	0	45.9
(e) AES—point 2 of Fig. 2	0	3.0	38.9	0	58.1
(f) AES—point 3 of Fig. 2	7.6	57.8	0	0	34.6

The values in rows (b) and (c) differ only with respect to the Fe concentrations. It has to be kept in mind, however, that XPS averages over a much larger area than probed by AES corresponding to Fig. 2. The most striking difference between the surface and the bulk lies in the tremendous surface enrichment of K, thus confirming the suggestion that this element is not dissolved in the magnetite crystals but segregates to the grain boundaries.

3.2. Partially Reduced Catalyst

The catalyst sample was treated within the XPS system in a $H_2 + N_2$ (3 : 1) mixture of 500 Torr at 620K for several days. The progress of reduction was followed by recording the Fe 2*p* core level which shifts and narrows in characteristic manner upon transformation into metallic iron (*21*). As shown previously (*21*), the oxidation state of the other metals (K, Al, Ca) does not change under these conditions of reduction. This procedure causes no complete reduction of the iron particles. It has to be concluded that at this stage a magnetite core is surrounded by a shell of metallic iron in a manner as proposed by Baranski *et al.* (*25*).

If the secondary electron image (Fig. 5) is now compared with Fig. 2, mainly topographical variations in the center of the left part (which exhibited a high K concentration, cf. Fig. 4) become apparent. The Auger maps for K and Fe as reproduced in Fig. 5 demonstrate that potassium now covers the iron parts more uniformly than before reduction (cf. Fig. 4). The dark areas in

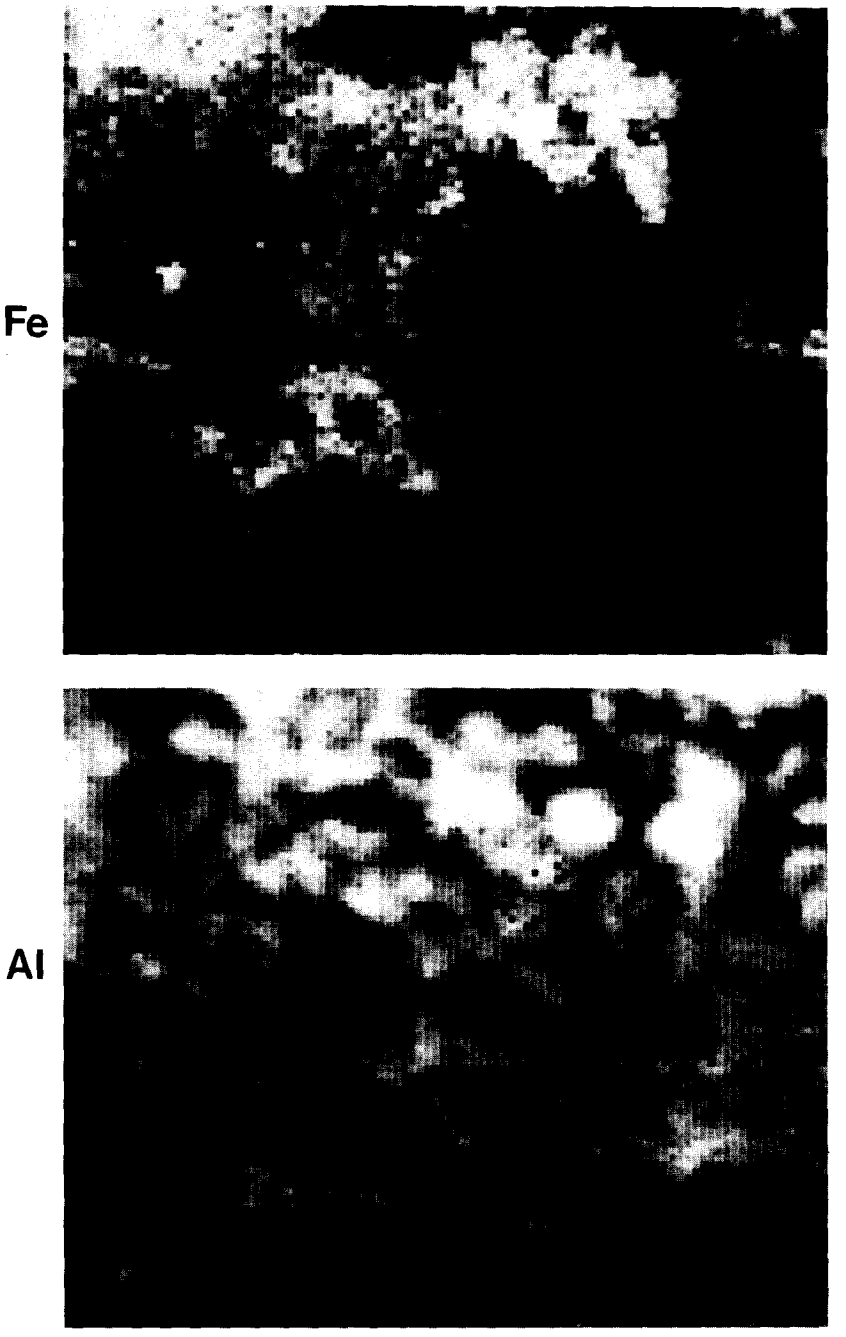

FIG. 4. "Auger maps" illustrating the lateral distributions of the elements Fe, K, Al, and Ca over the area whose SED image is reproduced in Fig. 2.

these maps consist essentially of Al_2O_3 and CaO. In addition, the overall surface concentration of Al has increased, which is consistent with the model whereafter Al_2O_3 being dissolved in the magnetite lattice segregates to the surface upon reduction.

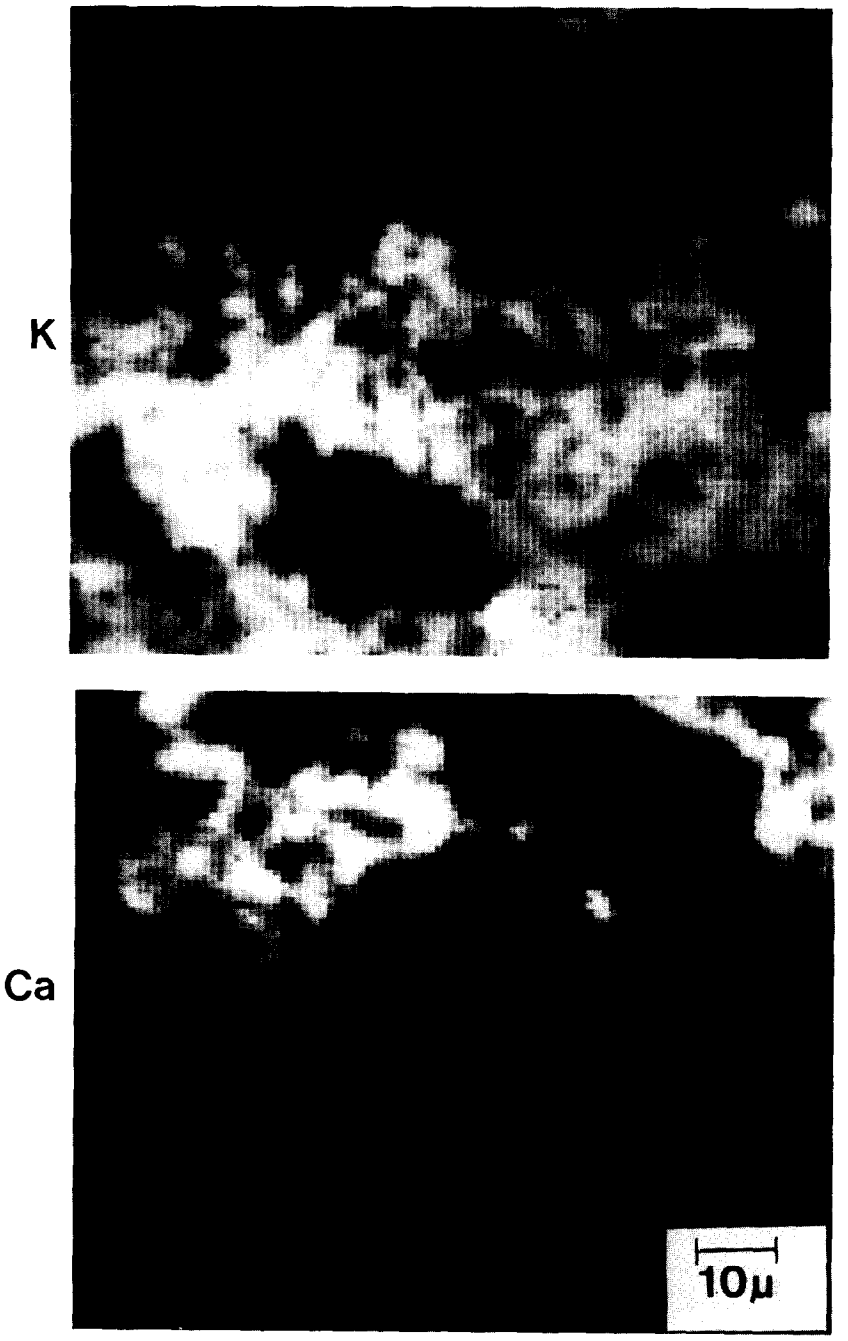

3.3. Reduced Catalyst

Complete reduction of the magnetite into metallic iron (as followed by XPS, i.e., within the probing depth of this technique) was achieved by prolonged treatment in the same $N_2 + H_2$ mixture as before, but now at the higher temperature of 720K.

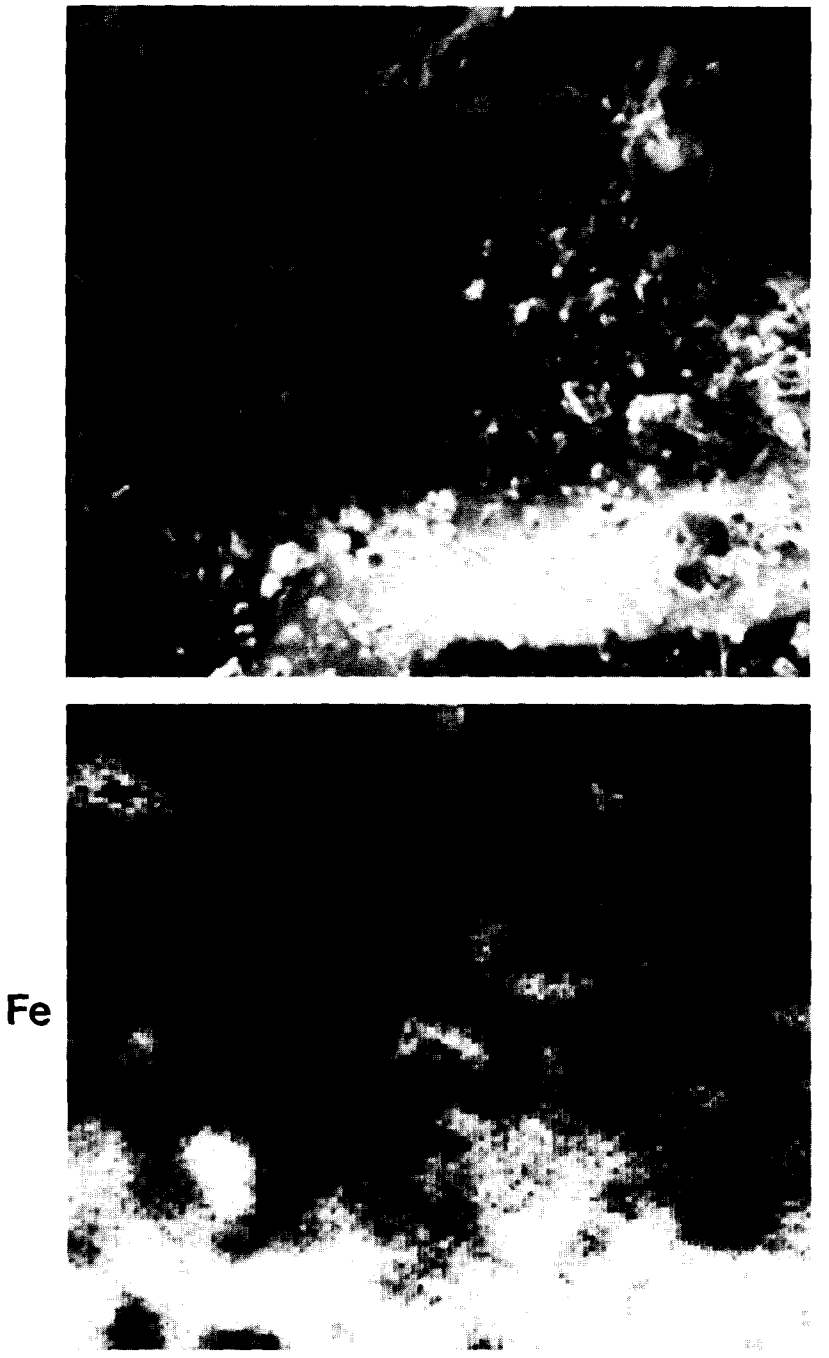

FIG. 5. SED image and Auger maps for Fe and K from the partially reduced catalyst surface (same area as in Figs. 2 and 4).

The secondary electron image (Fig. 6a) shows very little variation of the gross surface topography if compared with the partially reduced state (Fig. 5). Scanning electron micrographs taken with about the same magnification (Fig. 7) show the pres-

FIG. 5—*Continued.*

ence of crystallites on a rather "smooth" substrate, which on the other hand exhibits cracks which were caused by the reduction process. These smooth areas are, however, by no means structureless: high-resolution images (Fig. 8) show the formation of pronounced pore structure.

The catalyst particles with typical diameters around 300 Å form a rather open network with channels of about 100 to 500 Å in diameter. These figures have to be compared with the corresponding images before reduction (Fig. 3) and explain why the total surface area is now tremendously increased. (These features cannot be resolved with the scanning Auger electron spectrometer because of its limited resolution of ~500 Å.)

The lateral distributions of Fe, K, Al, and Ca on the surface of the fully reduced catalyst are reproduced in Fig. 9. These Auger maps have to be compared with corresponding data recorded from the same area of the unreduced (Fig. 4) and partially reduced (Fig. 5) catalyst. It becomes evident now that the iron particles are rather uniformly covered with a K(+ O) layer. This layer must be very thin, presumably only about a single atomic layer thick: mild Ar ion sputtering was found to drastically decrease the K concentration. In addition, the measured concentration of Fe below K would be much smaller if the overlayer would exhibit a thickness of ≥ 5 Å. The catalytically active Fe + K regions exhibit only a low Al content. Apart from this the originally present particles of Al_2O_3 do not exhibit essential variation in shape (compare Figs. 2 and 6a). CaO obviously shows a strong tendency for segregation.

The encircled region in Fig. 6a is reproduced with a magnified scale in Fig. 6b and exhibits the formation of a cubic crystallite. Point analysis revealed a high concentration of Al together with a small amount of Fe: this is obviously one of the various Al_2O_3/Fe_3O_4 spinel crystallites as identified by Peters *et al.* (*8*) by means of X-ray crystallography.

The results of a quantitative evaluation of

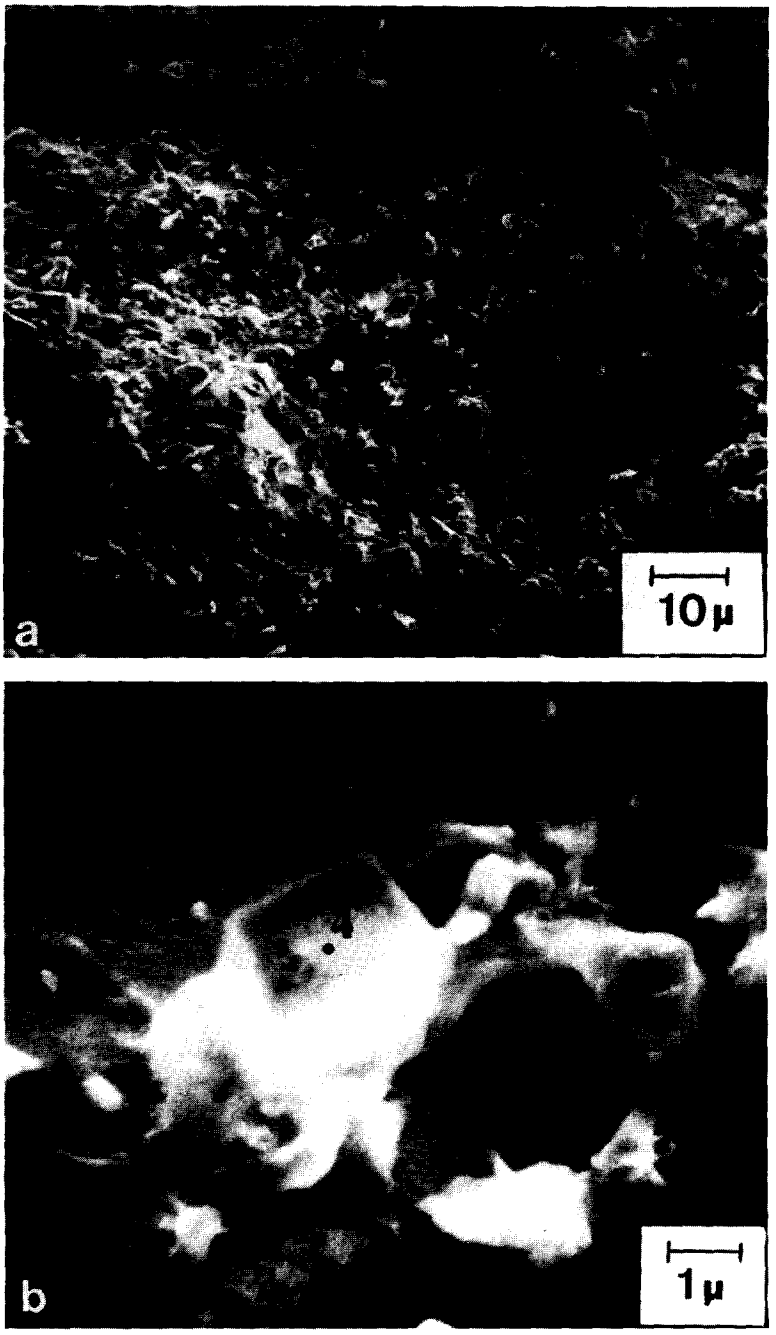

FIG. 6. (a) SED image from the same area as in Fig. 2 after complete reduction. The results of local AES analysis of the points 1–3 are listed in Table 2. (b) Enlarged-scale SED image of the area marked by a square in (a).

the surface compositions are summarized in Table 2. Comparison with Table 1 reveals that both XPS and AES indicate a pronounced increase of the integral Fe and Al concentrations, while that of K decreased and Ca remains essentially constant. For

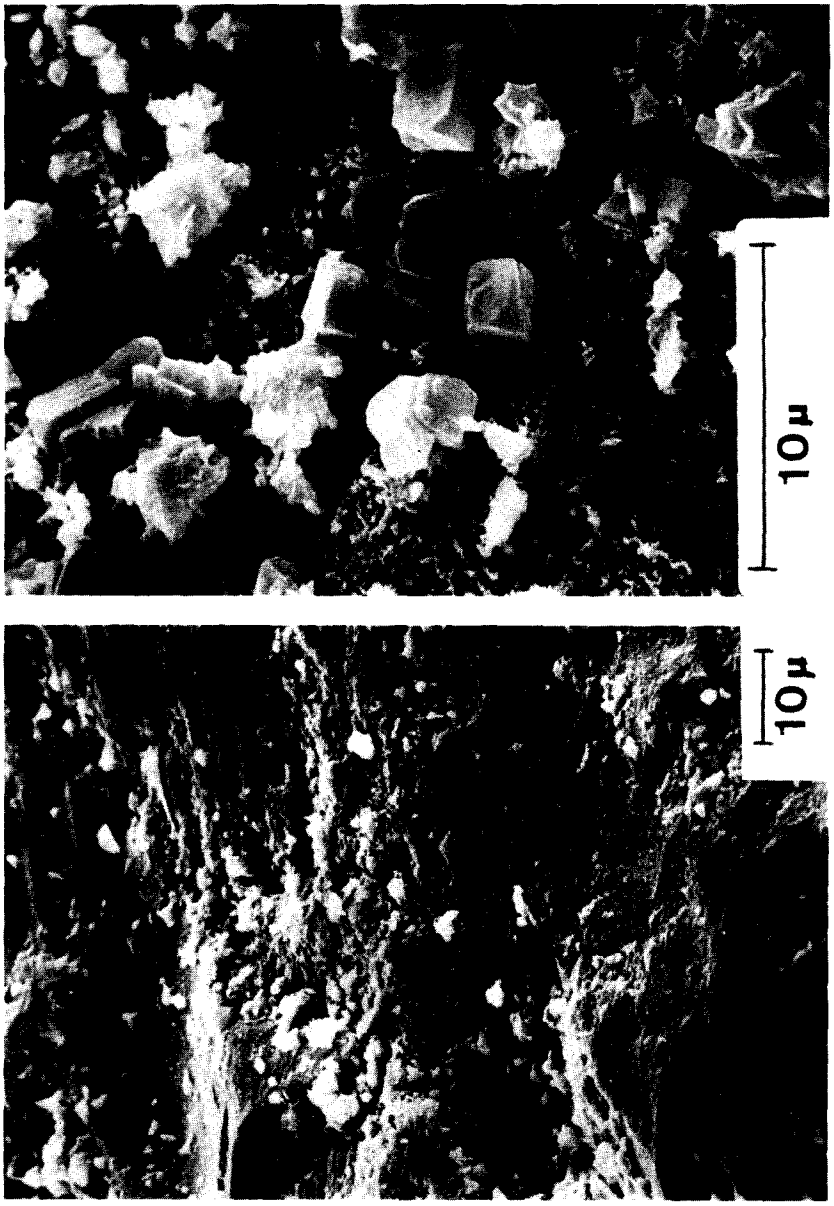

FIG. 7. Low-magnification SEM images from two selected areas of the reduced catalyst.

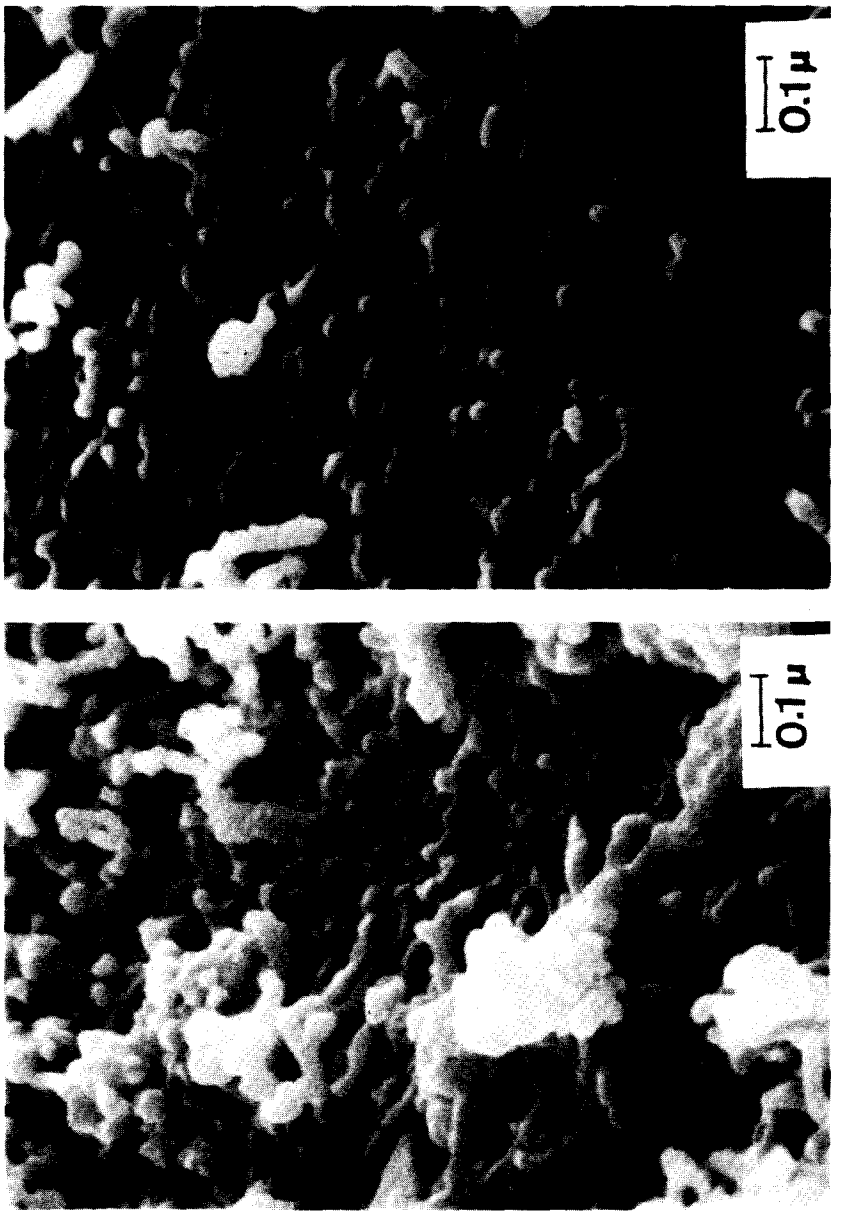

FIG. 8. High-resolution SEM images from the reduced catalyst showing the formation of rather uniform particles and pores.

TABLE 2

Composition of the Reduced Catalyst (at%)

	Fe	K	Al	Ca	O
XPS—total surface	6.4	24.2	16.3	4.1	49.0
AES—area of Figs. 2 and 6a	11.0	27.0	17.0	4.0	41.0
AES—point 1 of Fig. 6a	30.0	29.0	6.8	1.0	32.9[a]
AES—point 2 of Fig. 6a	—	13.1	—	40.4	46.5
AES—point 3 of Fig. 6a	—	5.3	37.5	2.4	54.8

[a] +0.3% S.

illustration of the inhomogeneous lateral distribution of the various elements a series of Auger spectra from four selected points (see Fig. 6) is reproduced in Fig. 10. Spectrum 1 originates from a typical catalytically active region and consists of about equal amounts of Fe and K plus some Al and a little Ca. Traces of S could only be detected on such Fe-rich areas.

4. DISCUSSION

The main findings of this study are in complete qualitative agreement with earlier conclusions in the literature and can be summarized as follows:

(i) The lateral distribution of the various elements in both the unreduced and the reduced catalysts is rather inhomogeneous. Similar conclusions were reached by Nielsen (*11*) and by Chen and Anderson (*12*) on the basis of electron microprobe analysis and by Hanji *et al.* (*22*) by applying Auger electron spectroscopy.

(ii) The unreduced catalyst exhibits essentially no pores with diameters <1000 Å. The reduced catalyst, on the other hand, is characterized by a network of pores with typical diameters in the range of ~100–500 Å as directly visualized by means of scanning electron microscopy.

On the basis of measurements with a mercury porosimeter, Peters *et al.* (*8*) concluded that a reduced catalyst containing 3% Al_2O_3 has a porosity of around 40–50%, and the pore distribution curve exhibits a maximum at pore diameters of around 400 Å. Nielsen (*11*) concluded on an average pore radius of 240 Å. These numbers depend, of course, on the composition and the conditions of reduction, but are exactly of the same order of magnitude as observed in the present study.

The nonreduced catalyst was found to exhibit only very large pores (2–10 μm), and the same holds for reduced magnetite, which contains no Al_2O_3 (*8*). The presence of 3% Al_2O_3, on the other hand, was found to increase the internal surface area by about a factor of 20. The BET surface of the reduced catalyst increases linearly with the Al_2O_3 content until a plateau at around 2.5%. There is therefore no doubt that Al_2O_3 acts as a "structural" promoter. A linear increase of the total surface area as well as of the free Fe surface (as determined by CO adsorption) with the degree of reduction was also observed with a magnesia promoted catalyst (*6*).

(iii) Reduction transforms iron completely into its metallic state. This becomes evident from the XPS data (*21*) and is in agreement with Mössbauer spectroscopic results (*18*), as well as with earlier determination of the lattice constant by X-ray diffraction, which was found to be exactly equal to that of α-Fe (*13*).

(iv) In the unreduced state the main fraction of Al_2O_3 is dissolved in the magnetite lattice, giving rise to a variation of the lattice constant (*26*), and part of the Al_2O_3 is segregated in the form of relatively large crystallites, as is evident from Figs. 2 and 4. After reduction aluminum is still rather homogeneously distributed over the iron areas. The following two possibilities can be discussed in order to explain the role of Al_2O_3 as structural promoter: (a) Upon reduction of Fe_3O_4 the dissolved Al_2O_3 segregates to the surfaces of the shrinking Fe particles and thus forms a rigid framework which prevents sintering, i.e., the gross volume remains unaffected. Schäfer (*10*) estimated that 3% Al_2O_3 would just be sufficient in order to cover the total internal surface of the reduced catalyst uniformly with about a monolayer of Al_2O_3.

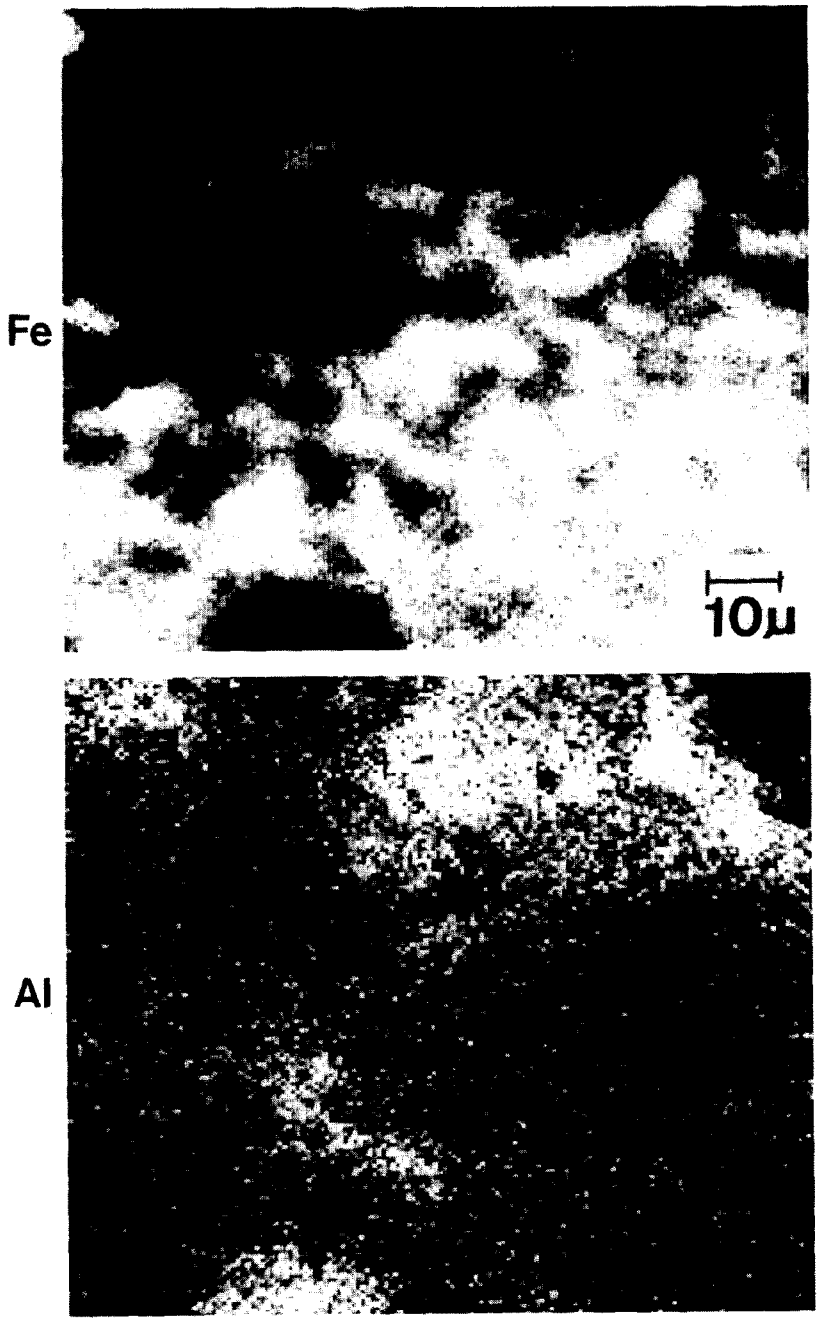

FIG. 9. Auger maps illustrating the lateral distribution of Fe, K, Al, and Ca after complete reduction (same area as in Figs. 2, 4, 5, and 6a).

The Auger data demonstrate that the surface region of the reduced Fe particles contain an appreciable Al concentration which cannot be "hidden" in the bulk because of the information depth of only a few Ångstroms of this technique. In contrast to the increase of the *total* surface area with increasing Al_2O_3 concentration the fraction of the total surface area being present as *free Fe surface* (as determined by selective CO

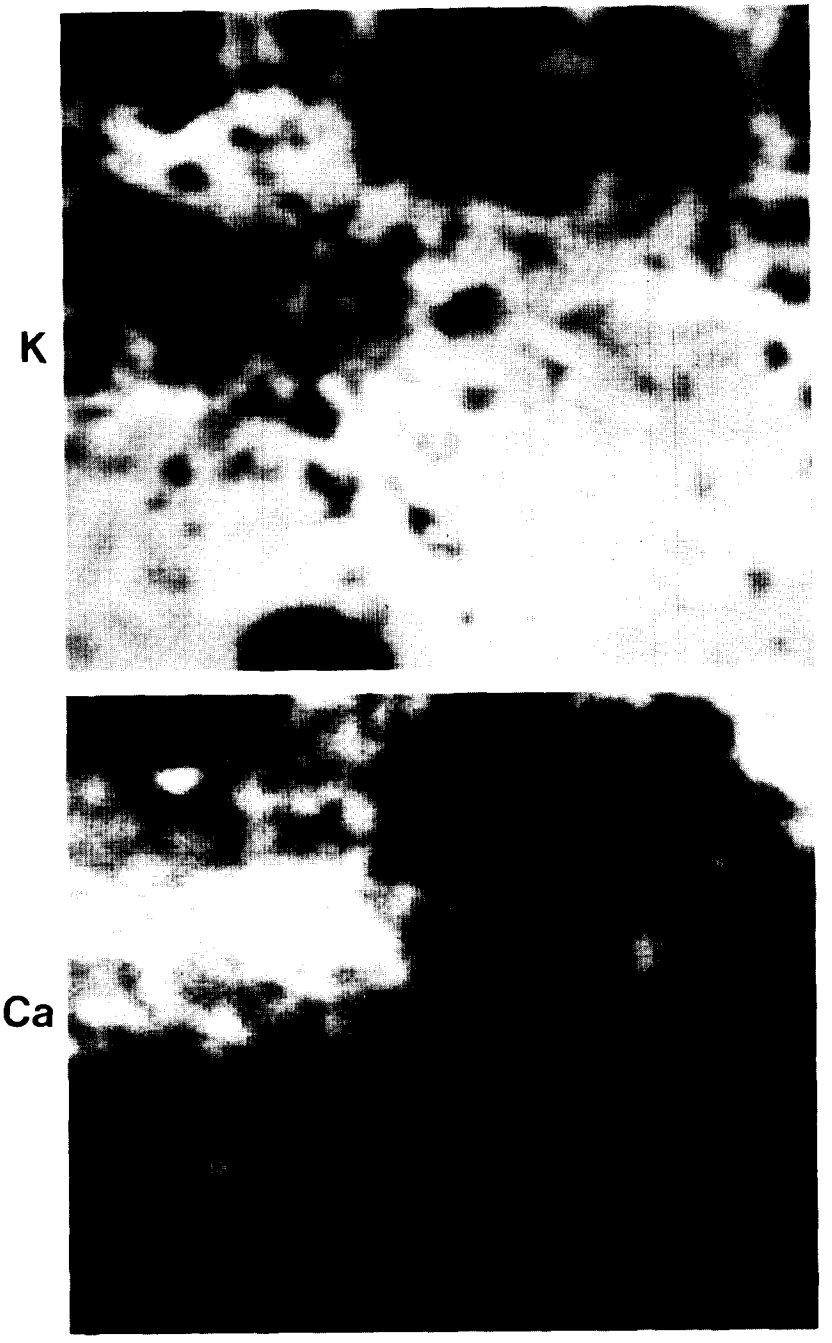

chemisorption) decreases continuously (*8*). This is considered to be a strong argument in favor of the model whereafter the Fe surface is partially covered with aluminum.

(b) The observed X-ray line broadening of the α-Fe crystallites was formerly ascribed to small particles, lattice strain, and faulting effects (*15*). More detailed analysis led, however, Hosemann *et al.* (*16, 17*) to the conclusion that this line broadening is

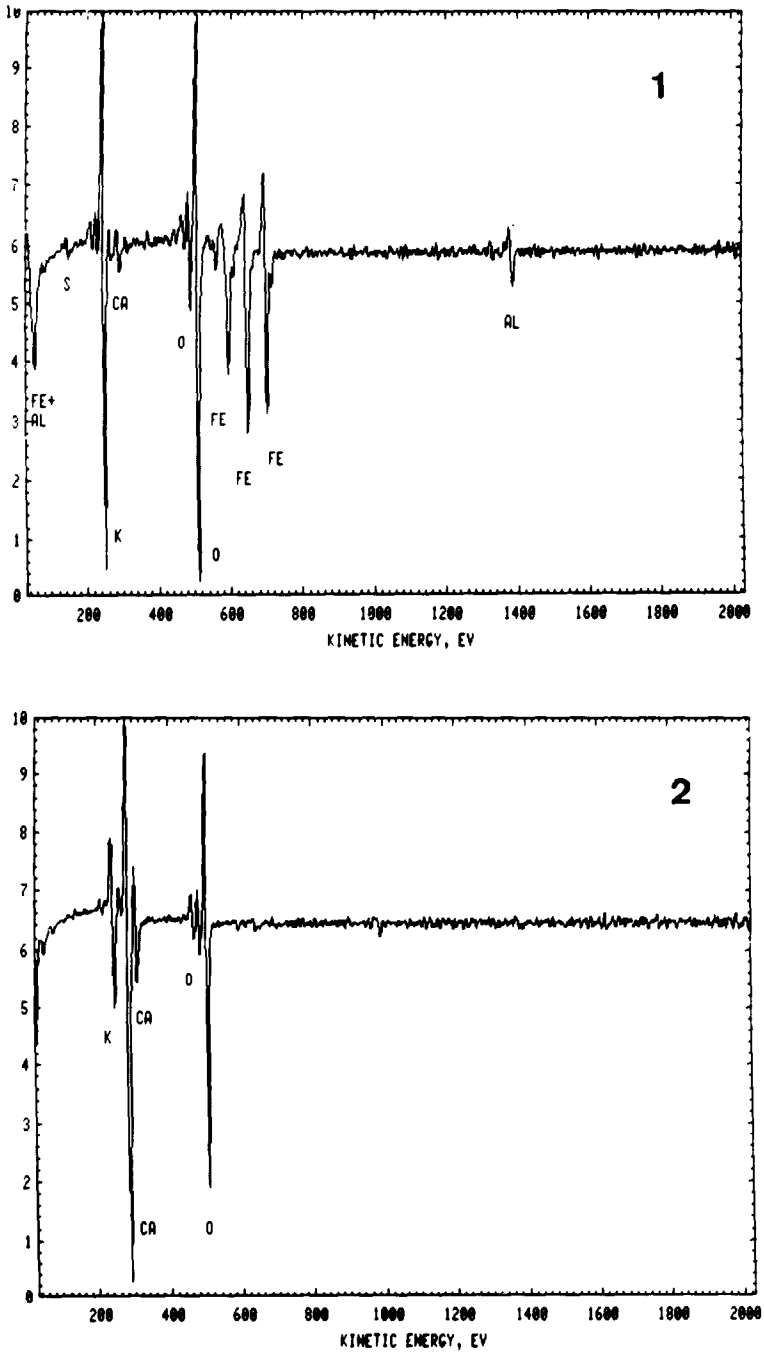

FIG. 10. Typical Auger electron spectra from four selected points (as marked in Fig. 6) of the surface of the reduced catalyst.

caused by a special type of long-range disorder denoted as "paracrystalline state." According to this view the high surface area of the alumina promoted catalyst is caused by the existence of these paracrystals which are prevented from sintering because

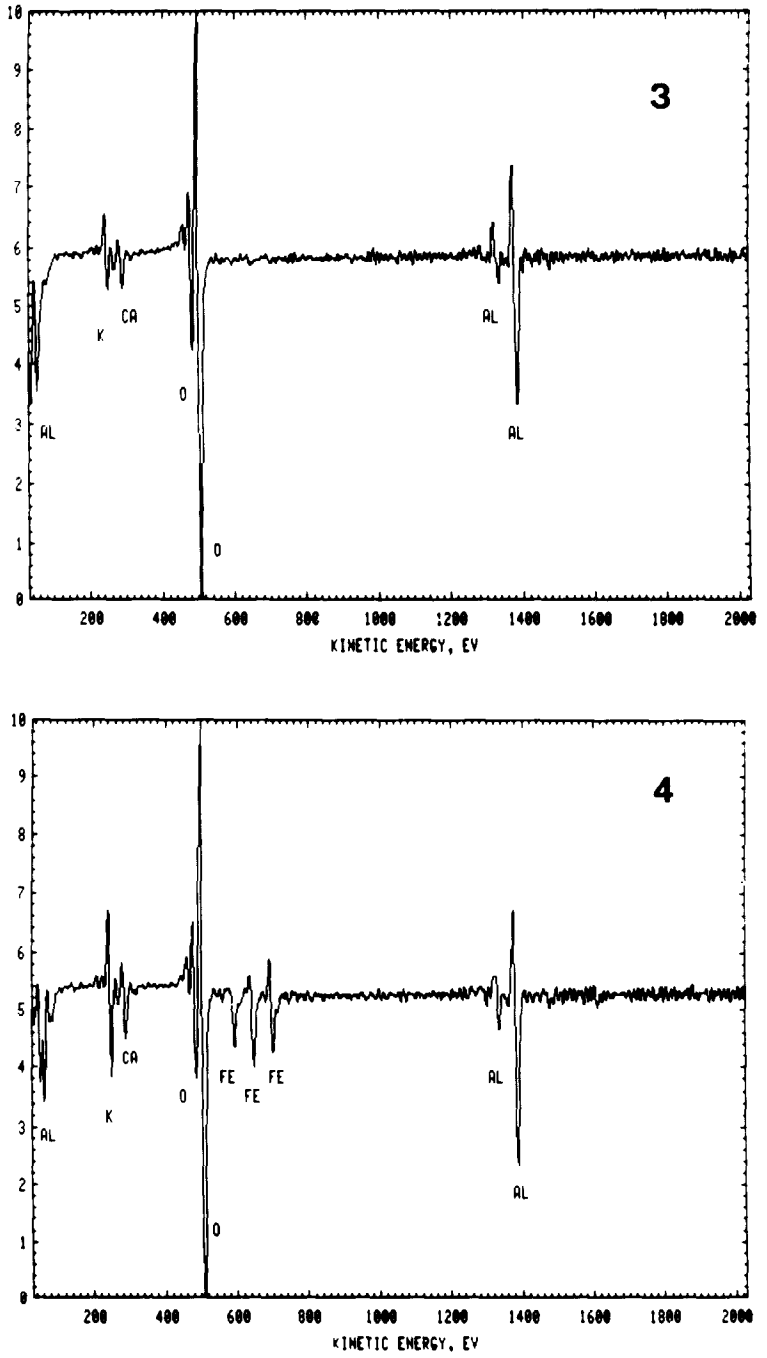

FIG. 10—*Continued.*

of internal distortions and which are formed by the presence of Al *inside* the Fe particles. It was suggested (*17*) that with magnetite crystals containing 3% Al_2O_3 and being reduced between 620 and 770K individual Al_2FeO_4 groups are endotactically built *into* the lattice of the α-Fe. The bulk content of Al would in this case be rather

small and would therefore cause no measurable variations of the electronic properties of the iron (as becomes evident from comparison of Mössbauer (*18, 19*) or XPS data with those from pure metallic Fe). Although this possibility cannot clearly be ruled out, it is difficult to reconcile it with the fact that certainly an appreciable amount of aluminum is on the surface, as becomes evident from the arguments of the preceding section.

(v) Potassium covers the Fe surface rather uniformly. On the basis of selective adsorption experiments (CO for Fe and CO_2 for K) Brunauer and Emmett (*3, 5*) had already concluded that the potassium promoter is finely distributed over the iron surface because preadsorbed CO_2 prevents subsequent adsorption of CO. Also the fractions of the total surface area due to Fe and K (and in particular the pronounced surface enrichment of potassium) determined by these methods (*5, 7, 9*) are in remarkably good agreement with the present findings. With a catalyst containing 0.5% K_2O in the bulk Krabetz and Peters (*9*) found, for example, that about 40% of the total surface is covered by potassium. Using a $H_2{}^{18}O$ isotope exchange technique led Solbakken *et al.* (*7*) to the conclusion that about 60% of the surface of a reduced catalyst (1% Al_2O_3 and 0.5% K_2O bulk content) is covered with the promoters.

The actual chemical nature and composition of the potassium layer is still under investigation in our laboratory. It is most probably not (bulk) K_2O nor any other of the known bulk compounds of potassium since these would become volatile under the relatively high temperatures of the synthesis reaction. Nielsen (*11*) concluded that K "must be bound to something else." The XPS data suggest that K + O form only a monoatomic layer on top of the Fe substrate. Previous model studies revealed that adsorbed K *alone* accelerates dissociative nitrogen adsorption (which is the rate-limiting step in ammonia synthesis) enormously (*27*), but would not be thermally stable (*28*). If, on the other hand, the surface is covered with a composite K + O adlayer, thermal desorption of potassium takes place only above reaction temperature ($\gtrsim$700K). Since adsorbed oxygen, however, poisons nitrogen adsorption it becomes plausible why the promoter effect of such a composite layer is rather modest (*28*), which is in qualitative agreement with the findings with "real" catalysts (*9*). Another parallelism is worth mentioning: with K adsorbed on Fe single crystals the activity for dissociative nitrogen adsorption passes through a maximum at a K coverage of about 40% of the monolayer capacity (*27*), while Krabetz and Peters (*9*) report on a maximum in catalytic activity if about 30% of the total surface area of a doubly promoted catalyst is covered by potassium (as determined by CO_2 adsorption). The results of a more detailed investigation on the thermal and chemical properties of the potassium overlayer on industrial ammonia synthesis catalysts will be published elsewhere (*29*).

(vi) CaO was found to segregate from the catalytically active Fe particles and therefore acts again as a structural promoter. It is reported (*9*) that addition of CaO increases the thermal stability against sintering, which is consistent with the topography of the distribution of this promoter.

ACKNOWLEDGMENTS

Financial support of this work by the Deutsche Forschungsgemeinschaft (SFB 128) and by the Fonds der Chemischen Industrie is gratefully acknowledged.

Note added in proof. After this manuscript was accepted for publication a paper by D. C. Silverman and M. Boudart, *J. Catal.* **77**, 208 (1982), appeared in which AES (however without scanning facilities) was used for gross surface analysis of ammonia synthesis catalysts. The reported surface compositions are in good qualitative agreement with the conclusions of the present work.

REFERENCES

1. A. Mittasch, DRP 254 437 (1910).
2. Recent reviews dealing with the characterization and properties of industrial ammonia synthesis catalysts: (a) Ozaki, A., and Akai, K., *in* "Cataly-

sis: Science and Technology" (J. R. Anderson and M. Boudart, Eds.), Vol. 1, p. 87. Springer-Verlag, New York/Berlin, 1981; (b) Nielsen, A., *Catal. Rev.* **23,** 17 (1981); (c) Boudart, M., *ibid.*, 1.

3. Emmett, P. H., and Brunauer, S., *J. Amer. Chem. Soc.* **59,** 310 (1937).
4. Emmett, P. H., and Brunauer, S., *J. Amer. Chem. Soc.* **59,** 1553 (1937).
5. Brunauer, S., and Emmett, P. H., *J. Amer. Chem. Soc.* **62,** 1732 (1940).
6. Hall, W. K., Tarn, W. H., and Anderson, R. B., *J. Amer. Chem. Soc.* **72,** 5436 (1950).
7. Solbakken, V., Solbakken, A., and Emmett, P. H., *J. Catal.* **15,** 90 (1969).
8. Peters, C., Schäfer, K., and Krabetz, R., *Z. Elektrochem.* **64,** 1194 (1960).
9. Krabetz, R., and Peters, C., *Angew. Chem.* **77,** 333 (1965).
10. Schäfer, K., *Z. Elektrochem.* **64,** 1190 (1960).
11. Nielsen, A., *Catal. Rev.* **4,** 1 (1970).
12. Chen, H. C., and Anderson, R. B., *J. Catal.* **28,** 161 (1973).
13. Brill, R., *Z. Elektrochem.* **38,** 669 (1932).
14. Dry, M. E., and Ferreira, L. C., *J. Catal.* **7,** 352 (1967).
15. Herbstein, F. H., and Smuts, J., *J. Catal.* **2,** 69 (1963).
16. Hosemann, R., Preisinger, A., and Vogel, W., *Ber. Bunsenges.* **70,** 796 (1966).
17. Ludwiczek, H., Preisinger, A., Fischer, A., Hosemann, R., Schönfeld, A., and Vogel, W., *J. Catal.* **51,** 326 (1978).
18. Topsøe, H., Dumesic, J. A., and Boudart, M., *J. Catal.* **28,** 477 (1973).
19. Fagherazzi, G., Galante, F., Garbassi, F., and Pernicone, N., *J. Catal.* **26,** 344 (1972).
20. Buhl, R., and Preisinger, A., *Surf. Sci.* **47,** 344 (1975).
21. Ertl, G., and Thiele, N., *Appl. Surf. Sci.* **3,** 99 (1979).
22. Hanji, K., Shimizu, H., Shindo, H., Onishi, T., and Tamaru, K., *J. Res. Inst. Catal. Hokkaido Univ.* **28,** 175 (1980).
23. "Handbook of Auger Electron Spectroscopy." Physical Electronics Industries, Eden Prairie, Minn., 1976.
24. Scofield, J. H., *J. Electron Spectrosc.* **8,** 129 (1976); Wagner, C. D., *Anal. Chem.* **44,** 1050 (1972).
25. Baranski, A., Bielanski, A., and Pattek, A., *J. Catal.* **26,** 286 (1972).
26. Estrik, R., *J. Chem. Phys.* **21,** 2094 (1953).
27. Ertl, G., Lee, S. B., and Weiss, M., *Surf. Sci.* **114,** 527 (1982).
28. Paál, Z. Ertl, G., and Lee, S. B., *Appl. Surf. Sci.* **8,** 231 (1981).
29. Prigge, D., and Ertl, G., in preparation.